Biochimica et Biophysica Acta 1827 (2013) 807–816

Contents lists available at SciVerse ScienceDirect

Biochimica et Biophysica Acta

journal homepage: www.elsevier.com/locate/bbabio

# Proteomic analysis of $F_1F_0$-ATP synthase super-assembly in mitochondria of cardiomyoblasts undergoing differentiation to the cardiac lineage

Elena Bisetto [a,1], Marina Comelli [a,1], Anna Maria Salzano [b], Paola Picotti [c], Andrea Scaloni [b], Giovanna Lippe [d], Irene Mavelli [a,e,*]

[a] Department of Medical and Biological Sciences, University of Udine, 33100 Udine, Italy
[b] Proteomics & Mass Spectrometry Laboratory, ISPAAM, National Research Council, 80147 Naples, Italy
[c] Institute of Biochemistry, Department of Biology, ETH Zürich, 8093 Zurich, Switzerland
[d] Department of Food Science, University of Udine, 33100 Udine, Italy
[e] M.A.T.I. Centre of Excellence, University of Udine, 33100 Udine, Italy

ARTICLE INFO

*Article history:*
Received 11 January 2013
Received in revised form 28 March 2013
Accepted 5 April 2013
Available online 12 April 2013

*Keywords:*
$F_1F_0$-ATP synthase
Supramolecular organization
$IF_1$
BN-PAGE
Cardiomyocyte-like differentiation
H9c2

ABSTRACT

Mitochondria are essential organelles with multiple functions, especially in energy metabolism. An increasing number of data highlighted their role for cellular differentiation processes. We investigated differences in ATP synthase supra-molecular organization occurring in H9c2 cardiomyoblasts in the course of cardiac-like differentiation, along with ATP synthase biogenesis and maturation of mitochondrial cristae morphology. Using BN-PAGE analysis combined with one-step mild detergent extraction from mitochondria, a significant increase in dimer/monomer ratio was observed, indicating a distinct rise in the stability of the enzyme super-assembly. Remarkably, sub-stoichiometric mean values for ATP synthase subunit e were determined in both parental and cardiac-like H9c2 by an MS-based quantitative proteomics approach. This indicates a similar high proportion of complex molecules lacking subunit e in both cell types, and suggests a minor contribution of this component in the observed changes. 2D BN-PAGE/immunoblotting analysis and MS/MS analysis on single BN-PAGE band showed that the amount of inhibitor protein $IF_1$ bound within the ATP synthase complexes increased in cardiac-like H9c2 and appeared greater in the dimer. In concomitance, a consistent improvement of enzyme activity, measured as both ATP synthesis and ATP hydrolysis rate, was observed, despite the increase of bound $IF_1$ evocative of a greater inhibitory effect on the enzyme ATPase activity. The results suggest i) a role for $IF_1$ in promoting dimer stabilization and super-assembly in H9c2 with physiological $IF_1$ expression levels, likely unveiled by the fact that the contacts through accessory subunit e appear to be partially destabilized, ii) a link between dimer stabilization and enzyme activation.


## 1. Introduction

Most of the cell energy is provided by mitochondria in the form of ATP through oxidative phosphorylation, whose final step is catalyzed by transmembrane ATP synthase ($F_1F_0$-ATP synthase) [1]. In bacteria, chloroplasts, and mitochondria, this enzyme functions to harness the energy of a transmembrane proton-motive force for ATP biosynthesis [2]. Its energy-coupling mechanism involves a rotary motion of the central stalk of the $F_1F_0$-complex driven by $H^+$ conduction through $F_0$ in the forward ATP synthesis direction, and an opposite $H^+$-pumping rotation backward driven by the free energy change of ATP hydrolysis [3–7]. In membranes, ATP synthase exists as a native functional dimer assembled to form long rows of oligomers [8]. Such ATP synthase self-association occurring constitutively in mitochondria promotes membrane curvature and formation of proper mitochondrial cristae ultrastructure [9–14]. In mammals, fewer data are available and the first projection structure of dimeric ATP synthase was solved by means of transmission electron microscopy and image analysis of the dimeric enzyme extracted from bovine heart in the presence of digitonin [15]. ATP synthase super-assembly is also considered to play a critical role in maintaining a high transmembrane potential, which ensures optimal conditions for an efficient ATP synthesis [8,16]. Consistently, increase in

*Abbreviations:* ATP synthase, $F_1F_0$-ATP synthase; BN-PAGE, blue native polyacrylamide gel electrophoresis; hrCN-PAGE, high resolution clear native polyacrylamide gel electrophoresis; $IF_1$, mitochondrial inhibitor protein; DMEM, Dulbecco's modified Eagle's medium; FCS, fetal calf serum; RA, all-trans-retinoic acid; C, parental H9c2 cells; D, differentiation-committed H9c2 cells; PBS, phosphate buffered saline; EDTA, ethylenediaminetetraacetic acid; Tris, tris (hydroxymethyl)aminomethane; EGTA, ethylene glycol-bis(β-aminoethylether)-N,N,N′,N′-tetraacetic acid; SDS, sodium dodecyl sulfate; Vm, $F_1F_0$-ATP synthase monomer; Vd, $F_1F_0$-ATP synthase dimer; Vo, $F_1F_0$-ATP synthase oligomer; SRM, Selected Reaction Monitoring mode; nanoLC–ESI-LIT-MS/MS, nano-liquid chromatography–electrospray-linear ion trap-tandem mass spectrometry; MS, mass spectrometry

* Corresponding author at: Department of Medical and Biological Sciences, University of Udine, p.le Kolbe 4, 33100 Udine, Italy. Tel.: +39 432 494350; fax: +39 432 494301.
*E-mail address:* irene.mavelli@uniud.it (I. Mavelli).
[1] These authors contributed equally to this work.

0005-2728/$ – see front matter © 2013 Elsevier B.V. All rights reserved.
http://dx.doi.org/10.1016/j.bbabio.2013.04.002

ATP synthesis was documented concomitant with increase in the formation of dimeric ATP synthase complexes also in mammalian cell lines [17]. In addition, by native electrophoresis analysis combined with in gel-activity measurements of bovine heart mitochondrial extracts we demonstrated that the ATPase activity of the enzyme dimer is greater than that of monomer at physiological temperature [18].

The overall structure of the mitochondrial ATP synthase monomer is well conserved from bacteria to humans. This enzyme is a multi-subunit complex formed by two functionally and physically coupled portions with dual genetic origin. Thus, ATP synthase biogenesis is a sophisticated process that depends on the coordinated expression of nuclear and mitochondrial genomes [19]. This enzyme presents a hydrophobic domain, $F_0$ (c-ring and a subunits), containing a $H^+$ channel, and a hydrophilic domain, $F_1$ ($\alpha_3\beta_3$ subunits), bearing the adenine nucleotide processing sites. $F_0$ and $F_1$ domains are connected by the so-called central (γ, δ, and ε subunits) and peripheral (b, d, OSCP, F6, A6L subunits) stalks [20]. Accessory subunits, which vary in different species, contribute to enzyme structure, regulation and supra-molecular organization. Their role in supra-molecular organization has been unveiled by native gel electrophoresis of the homodimeric enzyme, proteomic identification of dimer-specific subunits, and genetic deletion experiments in yeast, where removal of subunits e and g lead to a loss of the dimeric/oligomeric structures, together with a modification of mitochondrial cristae morphology [10,21–23]. A selective proteolysis approach applied to bovine heart mitoplasts allowed us to demonstrate a role of subunit e in dimer/oligomer stability even in mammals [24]. In addition, self-association of ATP synthase complexes was proved to occur through subunits of the lateral stalk [25,26] and subunits a and c of the $F_0$ sector [27], but the nature of the interface domains in monomeric/dimeric forms is still debated. In this context, the first 3D view by transmission electron microscopy at 27 Å of the yeast ATP synthase dimer [28] showed the existence of a narrow angle between monomers, in accordance with the first 2D image of the dimeric enzyme extracted from bovine heart [15]. On the other hand, three-dimensional maps of the ATP synthase dimer obtained using electron cryotomography of bovine [14] and yeast [29] mitochondrial membranes, revealing a V-shaped structure with a wider angle of 86° between monomers, have been reported more recently. The protein interface between monomers which interact within the membrane at the base of the peripheral stalks is elucidated, whereas the self-organization of ATP synthase dimers into rows, that is a requisite for normal cristae morphology, is reported as occurring without the need for direct protein contacts through dimers based on the highly variable distances and angles between dimers in a row [29]. Consistently, by large-scale molecular dynamics simulations the authors proposed that reduction in elastic energy of the membrane deformation caused by individual dimer is sufficient to drive the self-assembly of dimers into rows, thus emphasizing the key role of dimers in mitochondria morphology.

In mammals, endogenous mitochondrial inhibitor protein $IF_1$ [30], which plays a prominent role in enzyme activity regulation both in vitro and in vivo [31,32], has also been suggested to promote ATP synthase dimerization by formation of $IF_1$–$IF_1$ bridge [33]. Accordingly, it has been found that over- or reduced expression of $IF_1$ promotes or diminishes cristae formation in the mitochondria of cultured mammalian cells, respectively [17]. Recently, the atypical morphology of the syncytiotrophoblast mitochondria has been shown to correlate with a low content of dimeric enzyme and of $IF_1$, thus confirming a key role played by these elements in determining cristae shape in human placental mitochondria [34]. Nevertheless, whether or not $IF_1$ actually takes part in promoting ATP synthase dimerization still remains to be definitively demonstrated as dimer was observed in some cases even without bound $IF_1$ [35–37].

Cell energy demand changes dramatically during development and differentiation, and mitochondrial content and function can be adjusted to suit the current cellular status [38]. Thus, mitochondrial biogenesis is included in differentiation program to face phenotypes characterized by high energy demand, as for skeletal and cardiac myocytes. It was reported that, concomitant with mitochondrial biogenesis, coordinated changes in the metabolic enzymes of oxidative phosphorylation occur during myogenesis [39] and a significant increase in mitochondrial ATP synthase, including α and β subunits, is associated with adipogenesis [40]. Mitochondrial remodeling in term of maturation and network expansion occurs during cardiac differentiation of stem cells and cardiomyoblasts [41–43]; this process is considered as an essential mechanism toward the execution of the cardiac differentiation program [41,42]. In accordance, a recent analysis of different cardiac mesoangioblast populations illustrates that mitochondrial content in mesoangioblasts can have significant effects on their downstream potential for cardiac differentiation, and suggests that mitochondrial load could be utilized in a selection regime to purify the best candidates from a polyclonal population, for transplantation studies [44].

This study was aimed at investigating the ATP synthase supramolecular organization changes related to the mitochondrial biogenesis, and occurring in particular in H9c2 cardiomyoblasts committed to differentiation towards the cardiomyocyte lineage. Recently, we observed that organelle biogenesis concomitant with H9c2 cardiac-like differentiation involves a mass increase, changes in shape/structure (resulting in closely packed mitochondrial cristae), increased ATP synthase activity and augmented phosphorylating respiration, as well as enhanced whole $F_1F_0$-complex biogenesis [43]. By using blue native electrophoresis (BN-PAGE) [45] and MS-based proteomic analyses, here we have obtained evidence that ATP synthase super-assembly in mitochondria is also enhanced in cardiac-like differentiating H9c2, and that $IF_1$ plays a role in dimer stabilization. Such a role is probably unveiled by the fact that the monomer–monomer contacts through the accessory subunit e are partially destabilized. Dimer stabilization is accompanied by enzyme activation, through a mechanism still to be clarified, and is considered as a pre-requisite for the changes observed in cristae ultrastructure by favoring dimer rows formation.

## 2. Materials and methods

### 2.1. Cell cultures and differentiation treatments

Clonal cell line H9c2 was obtained from American Type Culture Collection (CRL-1446). Cells were grown at a density of about $10^5$ cells/cm$^2$ as monolayer in Dulbecco's modified Eagle's medium (DMEM) high glucose (Euroclone, Devon, UK), supplemented with 10% v/v fetal calf serum (FCS), 2 mM L-glutamine, penicillin (100 μU/ml), streptomycin (100 μg/ml) and gentamycin (10 μg/ml) (all from Euroclone). Subconfluent cells were committed to differentiate into the cardiomyocyte lineage by culturing in the presence of low serum (1% FCS) and 10 nM all-*trans*-retinoic acid (RA) (Sigma, St. Louis, MO, USA) [46]. Treatment was prolonged for at least 14 days [43]. Throughout treatment, the expression level of cardiac markers was evaluated to monitor the differentiating effects elicited and optimize the protocol reproducibility. Specifically, immunofluorescence microscopy was used with commercial antibodies for troponin 1 cardiac isoform (mouse monoclonal antibody, Abcam, Cambridge, UK), myosin heavy chain MHC (goat polyclonal antiboby, Santa Cruz Biotechnology Inc., Santa Cruz, CA, USA) and α-sarcomeric actin (mouse monoclonal antibody, Sigma). No positive signal for all the investigated markers was observed in the parental line.

### 2.2. Mitochondria isolation

Subconfluent parental (C) or differentiation-committed (D) cells were washed in phosphate buffered saline (PBS) (8.1 mM $Na_2HPO_4$, 1.4 mM $KH_2PO_4$, 137 mM NaCl, pH 7.4), proteolyzed with trypsin–

EDTA, centrifuged at 400 ×*g* for 5 min, at 25 °C, and suspended in homogenization buffer (250 mM sucrose, 10 mM Tris/HCl and 0.1 mM EGTA, pH 7.4), supplemented with 1:10 Sigma protease inhibitor cocktail (cat. P8340). Cell suspensions, at a concentration of $2 \times 10^7$ cells/ml, were sonicated in a ice-cold bath, attaining about 95% of disrupted cells. Mitochondria were isolated as described previously [43]. Briefly, cell homogenates were subjected to centrifugation (800 ×*g* for 12 min, at 4 °C) to remove intact cells, nuclei, and large cell debris. Pellets were washed for a total of three times, and the final supernatants were collected and centrifuged at 16,000 ×*g* for 20 min, at 4 °C, to obtain mitochondrial pellets. Mitochondria were finally suspended in isotonic buffer and immediately used or frozen at −80 °C and stored until further use. Protein content was determined according to the Lowry method [47].

### 2.3. Enzyme activity assays

#### 2.3.1. ATP synthase

The rate of ATP synthesis catalysed by the mitochondrial ATP synthase was measured monitoring the increase in absorbance at 340 nm using a hexokinase: glucose-6-phosphate dehydrogenase coupled enzyme system as in [43]. Briefly, freshly isolated intact mitochondria were suspended in 20 mM glucose, 10 mM HEPES pH 7.5, 50 mM KCl, 5 mM $MgCl_2$, 10 mM $KH_2PO_4$, 10 mM potassium succinate, 20 UI/ml hexokinase, 22 UI/ml mM glucose-6-phosphate dehydrogenase, 1.5 mM $NADP^+$, 30 U/ml lactate dehydrogenase (Boehringer Mannheim, Mannheim, Germany), 40 U/ml pyruvate kinase (Boehringer Mannheim) and allowed to incubate with gentle shaking at room temperature for 3 min. 20 mM P–P diadenosine-5′ pentaphosphate was also present to inhibit contaminant adenylate kinase. The reaction was initiated by adding Tris-buffered ADP (final concentration 5 mM). The selective measurement of ATP synthase activity was ensured on the basis of sensitivity to 10 μM oligomycin.

The rate of ATP hydrolysis catalysed by ATP synthase was measured following the decrease in absorbance at 340 nm, by using the pyruvate kinase: lactate dehydrogenase coupled ATP-regenerating enzyme system, as in [43]. Briefly, freshly-isolated mitochondria were osmotically shocked by 5-fold dilution in distilled water and incubated with 30 mM sucrose, 50 mM Tris–HCl (pH 7.4), 50 mM KCl, 2 mM EGTA, 4 mM $MgCl_2$ and 4 μM rotenone, for 15 min under gentle shaking. 2 mM phosphoenol pyruvate, lactate dehydrogenase (Boehringer, Mannheim) (30 U/ml), pyruvate kinase (Boehringer Mannheim) (40 U/ml) and 0.3 mM NADH were then added to the assay mixture and allowed to incubate for 3 min, at 25 °C, with gentle shaking. Reaction was initiated by adding Tris-buffered ATP (2 mM final concentration). Interferences by contaminant $Ca^{2+}$- and $Na^+$/$K^+$-ATPases were minimized due to the composition of the buffer (containing EGTA and <5 mM $Na^+$), as verified in the presence of the specific inhibitors, sodium orthovanadate or ouabain [48]. To further prove the specificity of ATPase activity of mitochondrial ATP synthase, aurovertin (2 μM) inhibitor was routinely used in control assays. 10 μM oligomycin was used to determine the oligomycin-sensitive ATPase activity, which corresponds to the activity of the correctly assembled $F_1F_0$-complex, able to synthesize ATP.

Activities were expressed as Units (μmol/min) per mg protein, and normalized to citrate synthase activity as a measure of specific activity

#### 2.3.2. Citrate synthase

The assay was performed spectrophotometrically as described previously [43]. Briefly, isolated mitochondria were permeabilized by sonication and added to the assay buffer (0.1 mM 5,5′-dithiobis-2-nitrobenzoic acid, 0.3 mM acetylCoA and 0.5 mM oxalic acid). The increase in absorbance at 412 nm was measured with a reference cuvette lacking oxalacetate to correct for background thiolase activity. Activity was expressed as Units (μmol/min) per mg protein.

### 2.4. Gel electrophoretic and immunoblotting analyses

#### 2.4.1. Sample preparation and native electrophoresis

Isolated mitochondria were diluted at the final protein concentration of 15 mg/ml in solubilization buffer (50 mM NaCl, 5 mM 6-aminocaproic acid and 30 mM Tris–HCl pH 7.4). Samples were solubilized with digitonin (Fluka, St. Louis, MO, USA) using a detergent to protein ratio ranging from 2 to 7 w/w in a final volume of 40 μl; they were immediately centrifuged at 100,000 ×*g* for 25 min, at 4 °C, recovering the soluble fraction. Protein concentration was determined according to the Bradford method [49]. Supernatants were supplemented with Coomassie blue G-250 (Serva, München, Germany) and BN-PAGE was carried out in gradient gels (4–11% acrylamide) according to previous studies [18,45]. Gels were stained with Coomassie blue G-250 or with *in-gel* activity staining [18], or subjected to immunoblotting (1D-BN-PAGE/immunoblotting), or to iterative SDS-PAGE-immunoblotting (2D BN-PAGE/SDS-PAGE/immunoblotting). Molecular mass of $F_1F_0$-ATP synthase dimeric (Vd) and monomeric (Vm) forms was estimated by using bovine heart mitochondria as a standard. The linearity of the band intensities observed after Coomassie staining and/or Western blot detection was verified by performing densitometric scanning of lanes loaded with increasing quantities of samples; ImageQuant, version 2003.03 (Amersham, Glattbrugg, CH) and Quantity One 4.2.1 (Bio-Rad, Berkeley, CA) software were used to this purpose.

#### 2.4.2. In-gel ATPase activity staining

BN-PAGE lanes of interest were incubated in 35 mM Tris–HCl pH 7.4, 270 mM glycine, 14 mM $MgSO_4$, 0.2% w/v $Pb(NO_3)_2$, 8 mM ATP at 30 °C, overnight. ATP hydrolysis correlated with the development of a white lead phosphate precipitate. Gels were washed in water to stop the reaction and scanned by densitometry against a dark background.

#### 2.4.3. Immunodetection of $IF_1$ in BN-PAGE-separated ATP synthase complexes and whole mitochondria

$IF_1$ immunodetection in whole mitochondria was performed by 1D-SDS-PAGE/immunoblotting. Mitochondria isolated from H9c2 cells were separated by 15% SDS-PAGE under reducing conditions [50] and analyzed for $IF_1$ and β subunits.

$IF_1$ immunodetection in ATP synthase complexes was achieved by 2D (BN-PAGE/SDS-PAGE) immunoblotting. Excised bands from BN-PAGE were separated by 2D glycine-SDS-PAGE under denaturing conditions using 15% polyacrylamide gels. Afterwards, proteins were stained with Coomassie Blue G-250 or analyzed for $IF_1$ and β subunits.

Gels were electrotransferred to nitrocellulose membrane (Biorad Hercules, CA, USA) using a semidry electroblotting system (Bio-Rad) and membranes were blocked in 20 mM PBS pH 7.4 containing 3% w/v non-fat dry milk (Bio-Rad) and 0.1% Tween 20 (Sigma). The antibodies used were anti-β subunit monoclonal antibody (1:1000 dilution, Abcam, Cambridge, UK) and anti-$IF_1$ monoclonal antibody (1:1000 dilution, Mitosciences, Eugene, Oregon, USA). Membranes were incubated with the primary antibody in PBS buffer, overnight, and washed thoroughly; immunoreactive bands were visualized by enhanced chemiluminescence assay (Pierce, Rockford, IL, USA) according to the manufacturer's instructions, using horseradish peroxidase-conjugated goat anti-mouse IgG (Pierce), at a dilution of 1:5000. Band intensities were measured by peak integration after densitometry analysis. For quantification purposes, calibration experiments were carried out by using purified bovine $F_1$ [51] and $IF_1$ [52], which were considered as proper standard proteins to determine $IF_1$–$F_1$ molar ratio in mitochondria from rat-derived cells, according to sequence homology criteria.

### 2.5. Mass spectrometry analysis

#### 2.5.1. Mass spectrometric quantification of $IF_1$ in BN-PAGE-separated ATP synthase complexes

For qualitative experiments, 1D BN-PAGE bands corresponding to dimeric (Vd) and monomeric (Vm) forms of ATP synthase, as purified from C and D cells, were *in-gel* reduced, S-alkylated and digested with sequencing-grade trypsin (Roche) (12.5 ng/μl), at 37 °C. Peptide digests were subjected to a desalting/concentration step on μZipTipC18 pipette tips (Millipore Corp., Bedford, MA, USA) and analyzed by nanoLC–ESI-LIT-MS/MS using a LTQ XL mass spectrometer (Thermo, USA) equipped with Proxeon nanospray source connected to an Easy-nanoLC (Proxeon, Odense, Denmark) [53]. For quantitative experiments, Vd and Vm bands were washed with 50 mM $NH_4HCO_3$, dehydrated in acetonitrile and digested with sequencing-grade endoprotease Lys-C (Roche) (20 ng/μl), at 37 °C. In this case, peptide digests were not subjected to a desalting step but directly analyzed by nanoLC–ESI-LIT-MS/MS, as reported above. In both cases, peptide mixtures were separated on an Easy $C_{18}$ column (10 × 0.075 mm, 3 μm) (Proxeon) using a gradient of acetonitrile containing 0.1% v/v formic acid in aqueous 0.1% v/v formic acid; acetonitrile ramped from 5% to 40% over 40 min, from 40% to 80% over 10 min and from 35% to 95% over 2 min, at a flow rate of 300 nl/min. Spectra were acquired in the range $m/z$ 400–2000. Acquisition was controlled by a data-dependent product ion scanning procedure over the three most abundant ions, enabling dynamic exclusion (repeat count 2 and exclusion duration 1 min). The mass isolation window and collision energy were set to $m/z$ 3 and 35%, respectively.

Raw data files from nLC–ESI-LIT-MS/MS experiments were searched with both MASCOT (version 2.2.06, Matrix Science, UK) and SEQUEST programs, within the Proteome Discoverer software package (Thermo Fisher, USA, version 1.0 SP1), against an updated UniProtKB rat non-redundant (2011/10/17 version) and/or an optimized ATPase subunit sequence database. A mass tolerance value of 2 Da (for precursor ion) and 0.8 Da (for MS/MS fragments), trypsin or endoprotease Lys-C as proteolytic enzyme, a missed cleavages maximum value of 2 and Met oxidation and Cys carbamidomethylation (only for qualitative experiments) as variable and fixed modifications, respectively, were used to this purpose. Candidates with an individual MASCOT score > 25 and/or with an individual SEQUEST score vs. charge state (CS) > 1.5 for CS 1, >1.9 for CS 2, >2.4 for CS 3, >3.3 for CS 4, corresponding to $p < 0.05$ for a significant identification, were further evaluated.

A relative quantification of $IF_1$ in Vd and Vm from both D and C samples was obtained by extracting and integrating, in the same nLC–ESI-MS total ion chromatogram, peak areas corresponding to a selected peptide from subunit $IF_1$, and a selected peptide from subunit γ or two peptides from subunit β, which were used as invariant references. Extracted ion chromatograms were calculated for the range $m/z$ 514.9–515.9, 657.4–658.4, 544.5–545.5 and 488.0–489.0 for peptide TREQLAALK ($IF_1$), ELIEIISGAAALD (γ), VVDLLAPYAK (β), and IGLFGGAGVGK (β), respectively. Peak areas were calculated by using the Genesis algorithm from Bioworks Qual Browser, version 2.0.7 (Thermo, USA). Relative percentage of $IF_1$ was then obtained by calculating the percentage ratio between peak area of $IF_1$ peptide and peak area of γ or β peptides.

#### 2.5.2. Direct quantification of γ and e subunits in ATP synthase complexes in digitonin-extracted mitochondria

For each of the two subunits, γ and e, a proteotypic peptide was chosen, based on existing shotgun datasets (data not shown) acquired on an Orbitrap mass spectrometer (Thermo, Bremen, Germany). Peptides VYGTGSLALYEK and YSYLKPR for subunits γ and e, respectively, were chosen to this purpose and their isotopically labeled synthetic AQUA versions were obtained from ThermoScientific (Ulm, Germany). In each peptide the C-terminal K or R residue was substituted with the corresponding deuterated version having a mass shift of +8 or +10 Da, respectively. Prior trypsinolysis, a known amount of the internal standard peptides was added to the protein mixtures, which were extracted from mitochondria of C and D cells with digitonin (used at a detergent/proteins ratio 3:1 w/w). In solution digestion and peptide clean-up were performed as previously described [24]. Peptide mixtures were analyzed on a 5500 QTrap mass spectrometer (AB/Sciex, Toronto, Canada) equipped with a nanoelectrospray ion source, operating in Selected Reaction Monitoring mode (SRM). Chromatographic separation of peptides was performed on a Tempo Nano LC system (Eksigent, Dublin, CA) coupled to a 15 cm fused silica emitter, 75 μm diameter, packed with a Magic $C_{18}$ AQ 5 μm resin (Michrom BioResources, Auburn, CA, USA). Peptides were loaded on the column from a cooled (4 °C) Eksigent autosampler and were separated with a linear gradient of acetonitrile/water, containing 0.1% formic acid, at a flow rate of 300 nl/min. A gradient from 5 to 30% acetonitrile in 30 min was used. Transitions corresponding to the doubly charged precursor of each peptide and all y-ions in $m/z$ 400–1250 were monitored. Transitions corresponding to fragments with $m/z$ values close to the precursor ion $m/z$ ($m/z_{Q1}$–$m/z_{Q3} \leq 10$ Th) were discarded. SRM acquisition was performed with Q1 and Q3 operating at unit resolution (0.7 $m/z$ half maximum peak width) and with a dwell time of 60 ms/transition. Collision energy (CE) was calculated according to the formula: $CE = 0.044 * m/z + 5.5$. Peak height for the transitions associated with the standard and endogenous peptides was extracted manually. Absolute quantification was obtained by calculating the ratio between the height of the SRM peaks derived from the light and heavy version of each peptide; results were expressed as the mean out of the different SRM transition traces.

### 2.6. Statistical analysis

Data are reported as means ± SD or SE Intergroup comparisons were made with Student's $t$-test for two groups. A value of $p \leq 0.05$ was considered to be statistically significant.

## 3. Results and discussion

### 3.1. Monomeric and dimeric ATP synthase in mitochondria of parental and differentiating cardiomyoblasts

BN-PAGE analysis was used to compare the supra-molecular assembly of ATP synthase in mitochondria from H9c2 cells committed to cardiac differentiation by chronic treatment with RA (D), with respect to the parental line used as control (C). To this purpose, sample extraction with digitonin ensured mitochondria solubilization without disrupting protein super-assembly. In both cell types BN-PAGE analysis resolved ATP synthase in its dimeric (Vd) and monomeric (Vm) forms (Fig. 1a, *left*), with both forms having ATPase activity (Fig. 1a, *right*), while no higher oligomeric forms were detected. As the proportion of the dimeric enzyme in BN-PAGE is strongly dependent on the amount of detergent used for extraction, we carefully evaluated (by densitometry of Coomassie blue-stained gel) the amount of Vd and Vm in C and D cells by extracting corresponding mitochondria with solubilization buffers having different detergent-to-protein quantitative ratios (Fig. 1b). Thus, we monitored the efficiency of solubilization together with the detergent-sensitivity of Vd, which is indicative of the aggregation state in membrane. Digitonin used at a detergent/protein ratio of 3:1 w/w was chosen as the experimental condition suitable for a better dimeric protein recovery in both cell types. Unfortunately, oligomer band intensities were near to detection limits, even when *hr*CN-PAGE analysis was performed at lower digitonin/protein ratio (data not shown), and poor resolution was obtained, likely due to low amounts of oxidative phosphorylation complexes in mitochondria from our cells. In this respect, it should be highlighted that structure/stability of high order oligomers is a widely debated question. While numerous

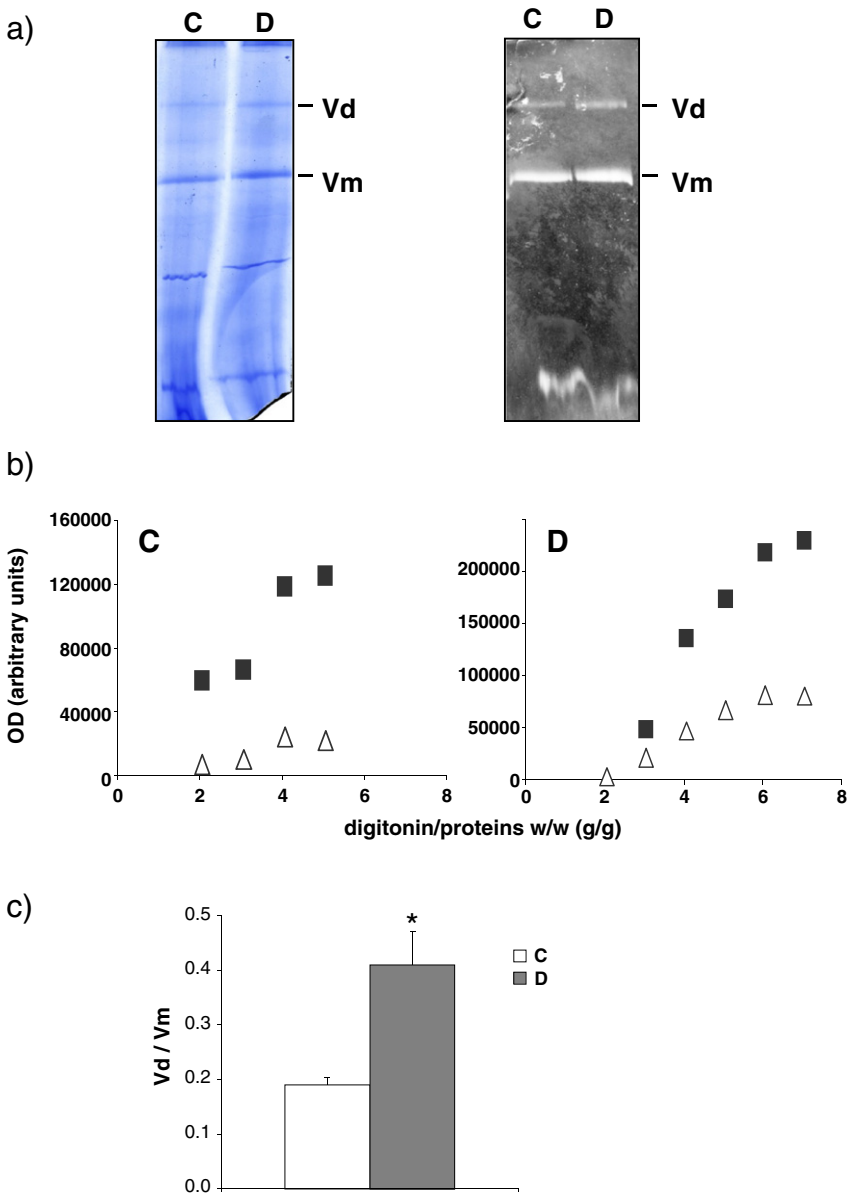


**Fig. 1.** Blue Native electrophoretic analysis of ATP synthase in control and differentiating mitochondria following extraction with digitonin. (a) Typical appearance of Coomassie blue G250-stained (*left*) and in-gel ATPase activity-stained BN-PAGE (*right*) of digitonin-extracted mitochondria. The position of ATP synthase dimeric (Vd) and monomeric (Vm) forms is indicated. This panel shows representative results from three independent experiments by performing digitonin extraction using a detergent/proteins ratio 3:1 w/w for both mitochondria types. (b) Mitochondria were treated with the indicated concentration of digitonin and analyzed by BN-PAGE. Values from densitometric analysis of dimer (Vd, empty triangle) and monomer (Vm, closed square) are reported (one experiment representative of three). Experimental condition for a better dimer recovery was detergent/mitochondrial proteins 3:1 w/w, which corresponded to minimal digitonin concentration to minimize monomer formation. (c) The dimer-to-monomer ratios (Vd/Vm), calculated from Coomassie blue-stained bands, are shown as a measure of the detergent-stability of Vd extracted with digitonin using a detergent/proteins ratio 3:1 w/w (white bar: mitochondria from parental control cells (C); gray bar: mitochondria from differentiation-committed cells (D). Values are the mean ± SE; $p \leq 0.01$ D vs. C, n = 3).

cross-linking studies supported the existence of a protein interface between dimers within oligomers, mainly through e/e and g/g subunits [54], evidence has been recently provided by electron cryotomography analysis of mitochondrial membranes and large-scale molecular dynamics simulations [29] that the dimers do not interact directly in membrane, with the self-assembly of dimers into rows depending on the membrane deformation caused by individual dimer. Such a view emphasizes the key role of dimers as a pre-requisite for mitochondria morphology and function. Based on such considerations, we are confident that for BN-PAGE analysis Vd/Vm is actually a proper index representing the stability of the overall ATP synthase super-assembly (i.e. the monomer–monomer contacts and the consequent self-assembly of dimers into rows, less stable to detergent extraction and BN-PAGE). A comparison of the Vd/Vm ratios computed for parental and differentiated cells demonstrated a meaningfully higher value for the latter (C: Vd/Vm ratio 0.19 ± 0.02; D: Vd/Vm ratio 0.41 ± 0.06; $p \leq 0.01$; n = 3) (Fig. 1c), suggesting that cardiomyogenesis may favor ATP synthase supra-molecular assembly in our model. Experiments reported in Fig. 1b also indicated a reduced sensitivity of the dimeric protein from D mitochondria to detergent action, which was suggestive of its greater stability.

To qualitatively evaluate protein composition, Vd and Vm forms from both cell types were subjected to classical proteomic analysis. Thus, corresponding gel portions were reduced, alkylated and digested with trypsin under standard conditions, and resulting peptide mixtures were analyzed by nLC–ESI-LIT-MS/MS. Table 1 reports the proteins identified in each ATP synthase band. As result of the poor gel cross-linking properties, various protein components were probably

**Table 1**
Qualitative analysis of ATPase subunits in Vm and Vd bands from digitonin-extracted mitochondria of C and D cells. Expasy accession number, protein name and sequence coverage are reported.

| Accession number | Protein name | Vm C cells coverage (%) | Vm D cells coverage (%) | Vd C cells coverage (%) | Vd D cells coverage (%) |
|---|---|---|---|---|---|
| P15999 | ATP synthase subunit alpha, mitochondrial | 51 | 59 | 61 | 67 |
| P10719 | ATP synthase subunit beta, mitochondrial | 63 | 75 | 63 | 67 |
| P35435 | ATP synthase subunit gamma, mitochondrial | 30 | 31 | 38 | 38 |
| P35434 | ATP synthase subunit delta, mitochondrial | 8 | 14 | 14 | 14 |
| Q06647 | ATP synthase subunit O, mitochondrial | 54 | 64 | 46 | 58 |
| P19511 | ATP synthase subunit b, mitochondrial | 41 | 52 | 33 | 41 |
| P31399 | ATP synthase subunit d, mitochondrial | 66 | 81 | 78 | 78 |
| P29419 | ATP synthase subunit e, mitochondrial | 61 | 70 | 46 | 46 |
| P11608 | ATP synthase protein 8 (A6L) | 31 | 31 | 34 | 34 |
| Q6PDU7 | ATP synthase subunit g, mitochondrial | 30 | 50 | 30 | 37 |

not retained during alkylation/extraction steps, thus determining the improper detection of specific low molecular mass ATP synthase subunits (including $IF_1$), as already reported in previous studies [55–57].

### 3.2. Quantitative mass spectrometry analysis of ATP synthase subunits in digitonin-extracted mitochondria

Digitonin-extracted mitochondria from C and D cells were directly analyzed in order to quantify the amount of specific ATP synthase subunits. To this purpose, we applied a targeted proteomic approach based on SRM mass spectrometry and labeled synthetic peptides (AQUA approach), which was previously validated by us for the complex extracted from bovine heart mitochondria [24]. Considering the crucial role documented for the subunit e in mitochondrial ATP synthase supramolecular organization both in yeast [10,22] and mammals [24], and based on the higher value of the dimeric protein observed in D mitochondria (see previous section), we focused on quantification of the amount ratio of the subunit e vs. γ. Subunit γ was used as a reference of known stoichiometry. We selected one representative peptide for each subunit (γ and e) to be quantified, based on the following criteria: i) the peptide has to be unique to the target protein; ii) it has to be devoid of amino acids prone to artifactual modification; iii) it has to show a good MS detectability, based on previous shotgun proteomic data. Thus, peptides VYGTGSLALYEK and YSYLKPR were chosen for subunits γ and e, respectively. Known amounts of corresponding heavy labeled versions ad hoc synthesized were then added to protein extracts from digitonin-treated C and D mitochondria, prior to tryptic digestion. A quantification of the endogenous peptides and their corresponding heavy counterparts was obtained in each sample by using SRM on a triple-quadrupole mass spectrometer [24]. Multiple SRM transitions per peptide were monitored and used for quantification purposes. Signal ratio between the heavy and light peptides was used to calculate the absolute amount of peptides originally present in the samples and, then, the amount ratio of the two proteins. No difference in the ratio was observed between the samples, despite of the increase in the Vd/Vm measured in D mitochondria (Fig. 1c). In fact, the measured ratio (e vs. γ) for C and D was 0.45 ± 0.08 (n = 3) and 0.48 ± 0.10 (n = 4), respectively. These results indicate a sub-stoichiometric mean value for subunit e in both parental and differentiation-committed cells, and suggest that the higher dimeric protein recovery observed in the latter cannot be ascribed to an enhanced assembly of subunit e.

### 3.3. Effect of $IF_1$ on ATP synthase complexes: dimer/oligomers stability and activity regulation

In order to validate BN-PAGE data based on Coomassie blue staining, we further analyzed ATP synthase complexes of digitonin-extracted mitochondria (detergent/protein ratio 3:1 w/w) from D and C cells by 1D-BN-PAGE/immunoblotting experiments using monoclonal antibody anti β subunit. Immunodetection confirmed the presence of Vd in both samples, with the signal being greater in D extracts, and visualized unassembled $F_1$ in C extracts (Fig. 2a). As result of an augmented sensitivity of this analysis, 1D-BN-PAGE/immunoblotting sometimes revealed just in D extracts two faint bands corresponding to higher oligomeric forms (Fig. S1). This reinforced the hypothesis of an increased stability of the super-assembled complexes in mitochondria of D cells. Nevertheless, higher oligomers were revealed hardly even at low digitonin/protein ratio, whereas when we analyzed bovine heart mitochondria in separate experiments they were well revealed according to high abundance of ATP synthase and elevated stability of the super-assembled complexes (Fig. S1).

Since $IF_1$ was not detected during proteomic analysis of the bands from BN-PAGE or crude digitonin-extracts, 1D-BN-PAGE/immunoblotting experiments were also performed with monoclonal anti $IF_1$ antibody. Such method allowed us to probe $IF_1$ in ATP synthase complexes (Fig. 2b). Unexpectedly, no signal was revealed in Vd of both samples. On the other hand, $IF_1$ signal was found at the position corresponding to unassembled $F_1$, even if $F_1$ band was visualized hardly possibly due to the lower immune-reactivity of antibody anti β with respect to that anti $IF_1$. This result was in line with the regulatory role of $IF_1$, which is well known to inhibit the ATP synthase working in reverse, both in vitro and in vivo, thereby counteracting the consequent energy waste [30–32]. Such a role may contribute to avoid futile ATP hydrolysis by the assembly intermediate $F_1$ in our cells (mainly in C cells), as already suggested for ρ° cells lacking mitochondria-coded subunits [57].

To further investigate on the occurrence of $IF_1$ in ATP synthase complexes and to evaluate whether its epitope was masked within the dimer, slices of native gel corresponding to Vd and Vm were excised and submitted to 2D SDS-PAGE, followed by immunoblotting with anti β and anti $IF_1$ antibodies (Fig. 3a). Quantitative levels of these proteins within ATP synthase complexes were then estimated by densitometry based on a calibration with bovine heart $IF_1$ and $F_1$ (Fig. 3b). A greater $IF_1/F_1$ ratio in Vd from mitochondria of D cells was revealed with respect to control (namely, D: 1.06 ± 0.09 vs. C: 0.46 ± 0.02; $p \leq 0.01$, n = 3) (Fig. 3c and d). In accordance, computed $IF_1/F_1$ ratio in Vm species also suggested a greater amount of bound $IF_1$ in D cells. In summary, 2D immunoblotting analyses highlighted an increased content of endogenous $IF_1$ in Vd of mitochondria from cardiac-like differentiating cells, and suggested that $IF_1$ may contribute to the increased stability of ATP synthase dimer observed in these cells.

To further confirm this phenomenon, additional experiments were performed by using an independent quantitative proteomic approach (see Materials and methods section for details). Thus, Vd and Vm bands from both cell types were washed with 50 mM $NH_4HCO_3$ and directly subjected to endoprotease LysC digestion. This experimental setup avoided reduced detection of $IF_1$ resulting from non-proper protein retention in gel knits during reduction/alkylation/extraction steps (see previous section). All gel particles were then extracted and digests analyzed by nLC–ESI-LIT-MS/MS. By extracting and integrating peak areas corresponding to a selected peptide from $IF_1$, a peptide from

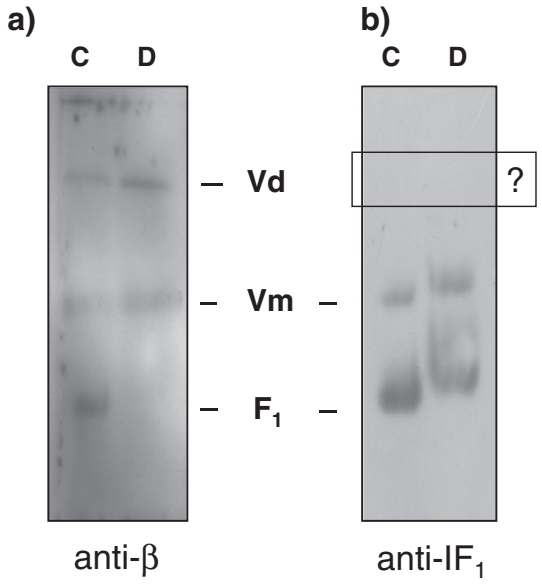


**Fig. 2.** Immunodetection of $IF_1$ bound in the ATP synthase complexes resolved in BN-PAGE: the dimer appears to lack $IF_1$. Control (C) and differentiation-committed (D) mitochondria were solubilized with digitonin using a detergent/proteins ratio 3:1 w/w and subjected to iterative 1D-BN-PAGE/immunoblotting with anti subunit β (a) and $IF_1$ (b) antibodies. The position of the dimer (Vd), monomer (Vm) and $F_1$ subcomplex is indicated. The panels show typical results representative of three independent experiments.

subunit γ or two peptides from subunit β in the same nLC–ESI-MS total ion chromatogram, a relative quantitative evaluation of $IF_1$ in the dimeric and monomeric ATP synthase forms from both cell types was obtained. Independently from the protein used as reference, histograms reported in Fig. 4 confirmed a quantitative trend for $IF_1$, as resulting from cell differentiation, similar to that reported in Fig. 3. Thus, 2D immunoblotting and MS analyses provided evidence in line with the hypothesis that $IF_1$ may participate in the enhancement of stability of ATP synthase dimer observed in a physiological range of $IF_1$ level, in accordance with the results of a recent study performed with human placental mitochondria [34].

Immunodetection of both $IF_1$ and β subunits was also carried out by 1D SDS-PAGE immunoblotting on mitochondria without separation by BN-PAGE or any other pretreatments. Results of quantitative analysis are shown in Fig. 5a and b. Considering the increased mitochondria mass in the D cells [43], values were referred to citrate synthase activity measured on lysed mitochondria, as a marker of mitochondria mass. Whereas a striking difference was observed in β subunit levels, which were higher in the D cells (in accordance with a greater amount of ATP synthase in the inner membrane), the levels of $IF_1$ were similar in mitochondria of both C and D cells. This finding indicates that the amount of $IF_1$, relative to the amount of its target molecule β subunit in $F_1$ sector, was higher in the parental cells, where conversely it was observed in less quantity as bound in the enzyme (Fig. 3c and d). These results suggest that $IF_1$ may represent a potential mechanism to provide a more rapid regulatory response in C cells, in line with the recognized regulatory role of $IF_1$. On the contrary, cardiac-like differentiating cells exhibited a greater steady-state amount of bound $IF_1$, which was in a molar ratio with $F_1$ sector close to 1:1 (Fig. 3c and d). Therefore, bound $IF_1$, contrary to the total levels of $IF_1$, appeared to augment along with the increase of the levels of β subunit in mitochondria during differentiation, and to parallel with the greater Vd/Vm ratio resolved by BN-PAGE of digitonin-extracts (Figs. 1 and 2), suggesting $IF_1$ binding as increasing along with $F_1F_0$-complex biogenesis and super-assembly.

Furthermore, we also investigated whether the different steady-state quantities of $IF_1$ bound to ATP synthase observed in mitochondria of C and D cells were affecting the enzyme activity. Fig. 5, panel c, shows the ATP synthase and oligomycin-sensitive ATPase maximal activities, measured by two coupled enzyme assays. Also in this case values were referred to citrate synthase activity to normalize the activities vs. mitochondria mass. Oligomycin-sensitive ATPase activity is a measure of the hydrolytic activity of the well coupled $F_1F_0$-complex, and it does not detect the activity of unassembled $F_1$ or of $IF_1$-inhibited $F_1F_0$-complex. Unexpectedly, markedly higher values were observed in D mitochondria for both ATP synthase and ATPase activities, regardless of the greater quantity of bound $IF_1$ (Fig. 2). Such increases were previously ascribed by us to the enhanced $F_1F_0$-complex assembly [43], but in light of the present data this cannot be the only reason, considering the greater quantity of bound $IF_1$ evocative of a greater inhibitory effect on the ATPase activity. This may suggest a contribution of $IF_1$-stabilized dimer in favoring a higher enzyme activity. As $IF_1$ seems not inhibitory but increases the ATP synthesis in cells with $IF_1$ overexpression [17], and mitochondrial proton motive force is augmented by $F_1F_0$-ATP synthase oligomerization [14,16], we may infer that the ATP synthase activity was increased in D mitochondria as a result of an increased local proton concentration due to stabilization of $F_1F_0$ supra-molecular assembly (Fig. 1 and 1-S) and cristae maturation [43]. On the other hand, even ATP hydrolytic activity was increased in D mitochondria, in line with our previous finding that the ATPase activity of dimer separated by BN-PAGE is greater than that of monomer at physiological

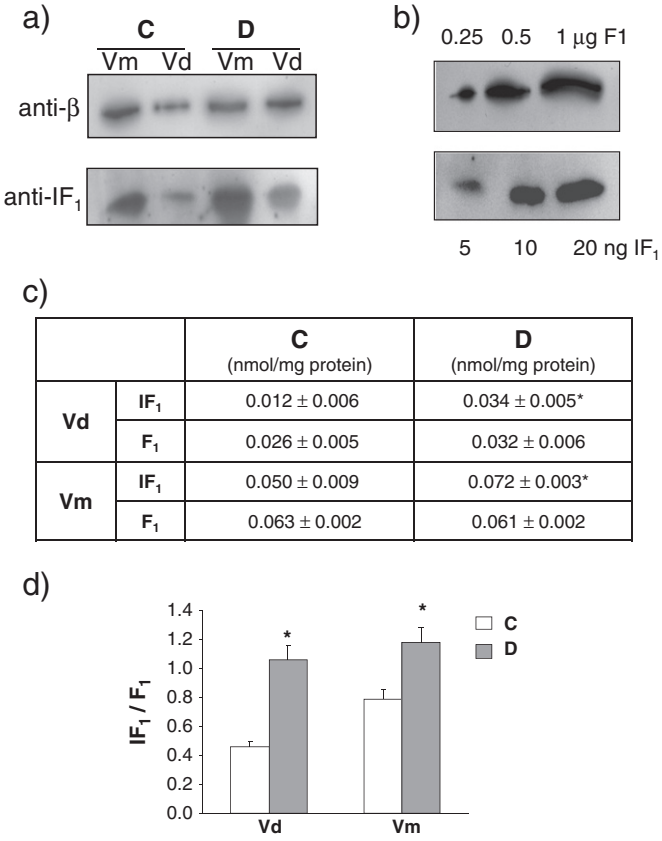


| | | C (nmol/mg protein) | D (nmol/mg protein) |
|---|---|---|---|
| Vd | $IF_1$ | 0.012 ± 0.006 | 0.034 ± 0.005* |
| | $F_1$ | 0.026 ± 0.005 | 0.032 ± 0.006 |
| Vm | $IF_1$ | 0.050 ± 0.009 | 0.072 ± 0.003* |
| | $F_1$ | 0.063 ± 0.002 | 0.061 ± 0.002 |

**Fig. 3.** Immunodetection of bound $IF_1$ in the ATP synthase under denaturing conditions. (a) 2D-SDS-PAGE/immunoblotting analysis of Vd and Vm cut out from BN-PAGE using anti ATP subunit β and anti ATP subunit $IF_1$ antibodies. (b) Reported quantities of bovine $F_1$ and $IF_1$ standards were used for quantification. (c) Mean ratios between the $IF_1$ subunit amount determined in Vd and Vm and that of the purified bovine $IF_1$ standard were measured; mean ratios between the β subunit amount determined in Vd and Vm and that of the purified bovine $F_1$ standard were measured. Values are the mean ± SE of three independent experiments; $p \leq 0.01$ D vs. C. (d) Molar ratios between $IF_1$ and $F_1$ in Vm and Vd are reported for control (white bars) and differentiation-committed cells (gray bars). Values are the mean ± SE of three independent experiments; $p \leq 0.01$ D vs. C.

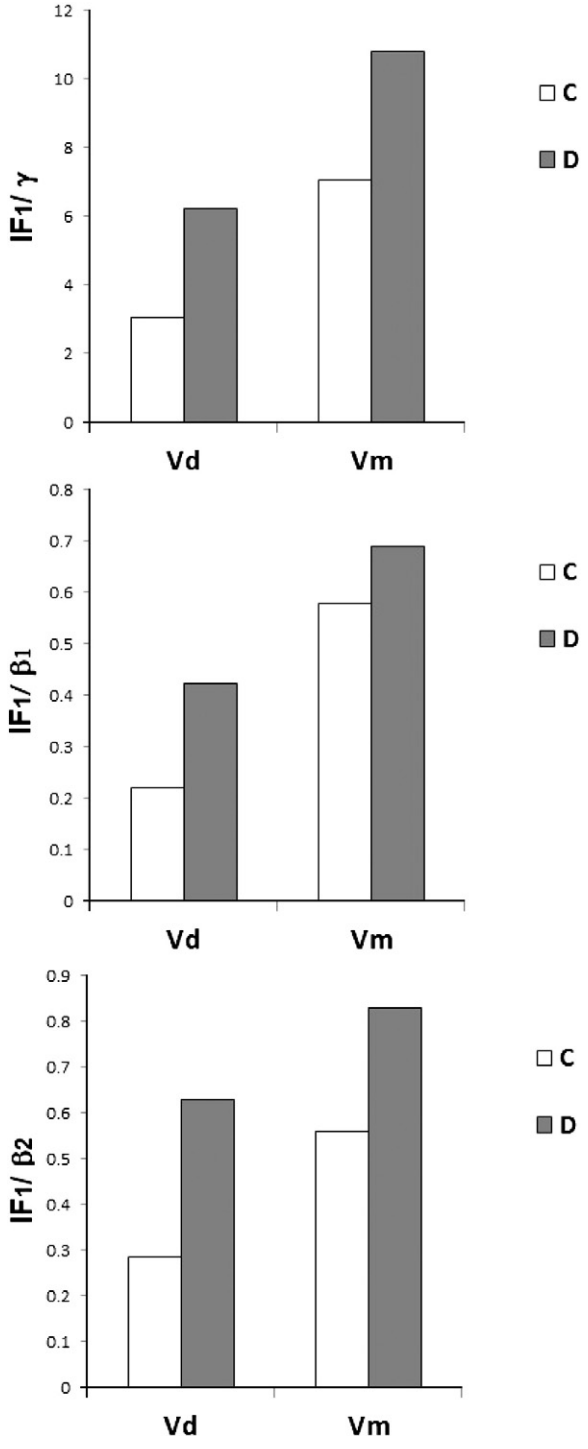


**Fig. 4.** Relative quantitative MS-based evaluation of $IF_1$ in monomeric and dimeric ATP synthase in mitochondria from parental and differentiating cells following extraction with digitonin. Experimental details are given in Materials and methods section. Relative quantification of $IF_1$ was obtained by extracting and integrating peak areas corresponding to peptides TREQLAALK ($IF_1$), ELIEIISGAAALD (γ), VVDLLAPYAK (β1), and IGLFGGAGVGK (β2) in the same chromatogram. Relative percentage of $IF_1$ was then obtained by calculating the percentage ratio between peak area of $IF_1$ peptide and peak areas of γ and/or β peptides.

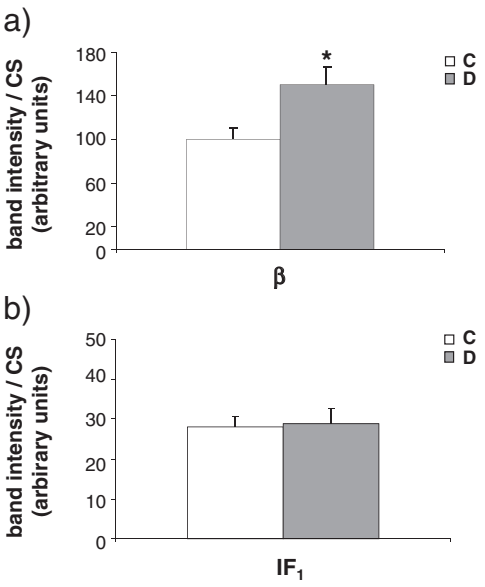


c)

| enzyme activity / CS | C | D |
|---|---|---|
| oligomycin–sensitive ATPase | 1.83 ± 0.24 | 3.65 ± 0.34* |
| ATP synthase | 1.25 ± 0.18 | 2.26 ± 0.28* |

**Fig. 5.** $IF_1$ and β subunit content in relation with the enzyme activity in mitochondria from parental and differentiating cells. (a, b) Quantitative immunoblot analyses were made for β and $IF_1$ subunits after 1-D SDS-PAGE of purified mitochondria from parental (C) and differentiation-committed (D) cells. Band intensities based on densitometry were normalized per mg protein and were related to citrate synthase activity. White and gray columns refer to C and D cells, respectively. For both proteins, values are the mean ± SD of four different experiments. *Significantly different with respect to control cells ($p \leq 0.01$). (c) The ATP synthase and the ATPase activities were determined by spectrophotometric assays performed respectively on intact (ATP synthase activity) and on osmotically-shocked (ATPase activity) mitochondria from C and D cells, as reported in Materials and methods. 10 μM oligomycin was used to determine the oligomycin-sensitive ATPase activity, which corresponds to the activity of the correctly assembled $F_1F_0$-ATP synthase, excluding the activity on unassembled $F_1$. The activities were normalized to citrate synthase activity. Data represent the mean ± SD of three different experiments. *Significantly different vs. parental control cells ($p \leq 0.01$).

temperature [18]. We conclude that $IF_1$-stabilized monomer–monomer contacts could have provided the enzyme with the ability to sustain a much more efficient ATP hydrolysis with a mechanism which remains to be clarified. In this regard, we advocate the hypothesis that $IF_1$ may stabilize the dimers as a result of a not-inhibitory binding, which may be in accordance with the recent V-shaped structure of dimer [14,29] with a distance between the two $F_1$ domains not consistent with the formation of an inhibitory $IF_1$–$IF_1$ bridge [33]. The stabilized dimer interface may favor rotor rotation during catalysis. Our finding that dimer bands were activity-stained (Fig. 1) but contained $IF_1$ in high molar ratio vs. $F_1$ may be in line with this hypothesis. A not-inhibitory binding anchoring $IF_1$ in the $F_1F_0$ complex in membrane was reported on bovine heart submitochondrial particles [58]. Nevertheless, we cannot exclude that, alternatively, ATP hydrolytic activity was $IF_1$-inhibited for the great fraction of $IF_1$-stabilized enzyme molecules, and a low fraction of the molecules did not contain $IF_1$ and was active. If this was the case, the catalytic efficiency of such molecules had to be greatly augmented. In this hypothesis, the overall supra-molecular assembly had to result more stabile and the dimeric structure of the $IF_1$-free active molecules also maintained.

## 4. Conclusions

The hypothesis that ATP synthase biogenesis has a crucial role in cardiac-like differentiation of H9c2 has been recently corroborated by BN-PAGE analysis focused on the assembly of $F_1F_0$-complex and carried out on mitochondria extracted with dodecylmaltoside [43]. Under such conditions, we documented a greater amount of the assembled $F_1F_0$-enzyme in mitochondrial membrane from cardiac-like

cells with respect to parental cardiomyoblasts, which conversely showed unassembled $F_1$ sub-complex in a greater extent. Differentiation was accompanied by mitochondria biogenesis and remodeling in terms of maturation of cristae, which appeared closely packed, and network expansion.

In this study, in order to characterize the super-assembly of ATP synthase, we applied a proteomic approach which was combined with the use of digitonin to solubilize mitochondria and to maintain dimeric/oligomeric complexes, as it is known that the combination of dodecylmaltoside with BN-PAGE dissociates dimeric ATP synthase into the monomeric form. Based on this approach, we may conclude that super-assembly of ATP synthase in mitochondrial membrane is favored during cardiomyogenesis, also suggesting a relationship between the acquisition of greater stability of supra-molecular organization and the mitochondria morphological modifications, i.e. cristae ultrastructure and network expansion. BN-PAGE analysis evaluated the proportion of dimer extracted from mitochondria, thereby demonstrating a higher dimer/monomer ratio in cardiac-like cells than in control, as a measure of a greater stability of the ATP synthase supra-molecular assembly. Quantitative mass spectrometry analysis on subunit e in digitonin-extracted ATP synthase suggested a negligible contribution of this subunit in the improvement observed in ATP synthase supra-molecular organization. Interestingly, the sub-stoichiometric mean value found for subunit e in both parental and differentiation-committed cells indicated a similar proportion of complex molecules lacking subunit e in both cases. This is difficult to be explained, due to scarcity of data on the assembly of the accessory subunits, like e subunit, in the process of ATP synthase biogenesis [59]. Nevertheless, it may indicate that the increase in β subunit content occurring during differentiation does not necessarily result in our model in the assembly of enzyme complexes containing all the 15 different subunits [60]. Unfortunately, BN-PAGE was not able to resolve the uncompleted complexes lacking e subunit, in accordance with the small differences expected in their molecular mass values. In conclusion, due to the well known role of subunit e in self-association of ATP synthase [10,22–24], this finding suggests that the super-assembled complexes lacking e subunit were not sufficiently stable for detergent-isolation, consistent with the low amounts of dimer/oligomer observed in digitonin-extracted mitochondria from H9c2 cells. Yet, the acquisition of greater stability of supra-molecular organization occurred in cardiac-like H9c2 had to be likely due to some other factors.

In this regard, we further investigated the controversial role of the mitochondrial inhibitor protein $IF_1$ in promoting the dimer stability in membrane. We quantified $IF_1$ by iterative BN-PAGE /2D SDS PAGE and immunoblotting using anti-$IF_1$ antibody, and confirmed the data by MS/MS quantification of $IF_1$ in ATP synthase complexes separated by BN-PAGE. We found a more marked amount of $IF_1$ associated to dimer in cardiac-like differentiating cells, as compared to the parental cells. Together, our present results confirm a role for bound $IF_1$ in promoting dimer stability and overall supra-molecular assembly, thereby favoring a higher enzyme activity. The hard resolution of higher oligomers on native gel may be explained by the lack of direct dimer–dimer contacts mediated by interstitial proteins [29], which prompt us to believe that the stabilization of monomer–monomer contacts by $IF_1$ is likely to favor in turn the self-assembly of dimers into rows in membrane, although these are less stable to detergent extraction and native electrophoresis, Such a role for $IF_1$ is in accordance with data from several independent laboratories [17,33,34,57], but in apparent divergence with others including our previous data [35–37]. These apparently conflicting results may be explained on the basis of the differences in type/abundance of the mitochondrial membranes investigated and/or in the experimental conditions used for solubilization of ATP synthase complexes [27]. In this regard, based on our present data of subunit e quantification, we hypothesize that the stoichiometry of the accessory subunits contributing to enzyme supra-molecular organization, such as subunit e, may play a role in unveiling the $IF_1$ effect on dimer stability. Indeed, in Triton-extracts of bovine heart mitochondria, which contained both subunit e [24] and $IF_1$ [18,35] in a molar ratio of ~1 with respect to $F_1$, we previously found that $IF_1$ removal did not significantly decrease the dimer content [35]. Conversely, in digitonin extracts of mitochondria from differentiated H9c2 cells, in which ATP synthase contained sub-stoichiometric subunit e but equimolar $IF_1$ (normalized to $F_1$), bound $IF_1$ appeared to improve dimer stability. However, it can't be excluded that the experimental conditions used for solubilization of ATP synthase complexes partially affected the results [27]. Based on these considerations, our present data prompt us to speculate that ATP synthase dimer may be formed even in the absence of $IF_1$, but the binding of $IF_1$ plays an important part in dimer stabilization especially if the monomer–monomer contacts through accessory subunits, or $F_0$ subunits, are partially destabilized. Consistent with this view, a fundamental role of $IF_1$ in dimer formation was postulated in $\rho_0$ cells lacking the $F_0$ subunits a and A6L [57]. However, the way by which $IF_1$ can stabilize the dimers and favor a higher enzyme activity is far to be elucidated, especially considering the still controversial descriptions of their structures [14,15,28,29].

Of note, our data have been obtained on a normal, non tumor, cell line in a physiological range of $IF_1$ level, and suggest that the enzyme activation mediated by stabilization of super-assembly via $IF_1$ binding to dimer may be a physiological response associated to cardiac-like differentiating conditions, which may be of more extensive importance. Indeed, such effects are not conflicting with the opposite effect elicited by $IF_1$ over-expressed at a very high level, which has been recently shown as resulting in ATP synthesis inhibition and associated to the intriguing mechanisms and signaling pathway by which $IF_1$ may participate in the biology of cancer cells [61]. It should be emphasized that the actual state of the art of ATP synthase supra-molecular organization was reviewed very recently [54], and the need was highlighted to further investigate the possibility that the relationship between cristae morphogenesis and ATP synthase super-assembly is conserved in mammalian cells and is associated with physiological consequences. In our opinion, H9c2 cardiomyoblasts and their counterparts induced to cardiac-like differentiation represent an interesting in vitro model of physiological modulation of cell conditions, where we attempted to characterize ATP synthase super-assembly in relation to cristae morphogenesis.

In conclusion, we demonstrate that $IF_1$ may provide an important but not exclusive contribution to ATP synthase dimer stability and super-assembly, thereby improving the enzyme catalysis efficiency. Such a contribution is expected to depend on the assembly of the enzyme accessory subunits participating to the supra-molecular organization, and specifically of subunit e which greatly varies with cell types, tissues and physio/pathological conditions [24].

Supplementary data to this article can be found online at http://dx.doi.org/10.1016/j.bbabio.2013.04.002.

## Acknowledgements

We are grateful to Dr. Stefania Contessi for her contribution in standard protein purification. This work was supported by the Italian Ministero dell'Istruzione, dell'Università e della Ricerca Scientifica (MIUR) grants (PRIN 2007 and Italian Human ProteomeNet Project 2007).

## Conflict of interest

None declared.

## References

[1] M. Saraste, Oxidative phosphorylation at the fin de siècle, Science 283 (1999) 1488–1493.

[2] P.D. Boyer, The binding change mechanism for ATP synthase, some probabilities and possibilities, Biochim. Biophys. Acta 1140 (1993) 215–250.
[3] P.D. Boyer, The ATP synthase—a splendid molecular machine, Annu. Rev. Biochem. 66 (1997) 717–749.
[4] R.A. Capaldi, R. Aggler, Mechanism of the F1F0-type ATP synthase, a biological rotary motor, Trends Biochem. Sci. 27 (2002) 154–160.
[5] B.A. Feniouk, M. Yoshida, Regulatory mechanisms of proton-translocating F(0) F(1)-ATP synthase, Results Probl. Cell Differ. 45 (2008) 279–308.
[6] S. Wilkens, Rotary molecular motors, Adv. Protein Chem. 71 (2005) 345–382.
[7] J.J. García-Trejo, E. Morales-Ríos, Regulation of the F1F0-ATP synthase rotary nanomotor in its monomeric-bacterial and dimeric-mitochondrial forms, J. Biol. Phys. 34 (2008) 197–212.
[8] M. Strauss, G. Hofhaus, R.R. Schröder, W. Kühlbrandt, Dimer ribbons of ATP synthase shape the inner mitochondrial membrane, EMBO J. 27 (2008) 1154–1160.
[9] J. Velours, A. Dautant, I. Sagot, D. Brethes, Mitochondrial F1F0-ATP synthase and organellar internal architecture, Int. J. Biochem. Cell Biol. 41 (2009) 1783–1789.
[10] P. Paumard, J. Vaillier, B. Coulary, J. Schaeffer, V. Soubannier, D.M. Mueller, D. Brèthes, J.P. di Rago, J. Velours, The ATP synthase is involved in generating mitochondrial cristae morphology, EMBO J. 21 (2002) 221–230.
[11] H. Yao, R.A. Stuart, S. Cai, D.S. Sem, Structural characterization of the transmembrane domain from subunit e of yeast F1Fo-ATP synthase: a helical GXXXG motif located just under the micelle surface, Biochemistry 47 (2008) 1910–1917.
[12] R.D. Allen, C.C. Schroeder, A.K. Fok, An investigation of mitochondrial inner membranes by rapid-freeze deep-etch techniques, J. Cell Biol. 108 (1989) 2233–2240.
[13] R.D. Allen, Membrane tubulation and proton pumps, Protoplasma 189 (1995) 1–8.
[14] K.M. Davies, M. Strauss, B. Daum, J.H. Kief, H.D. Osiewacz, A. Rycovska, V. Zickermann, W. Kühlbrandt, Macromolecular organization of ATP synthase and complex I in whole mitochondria, Proc. Natl. Acad. Sci. U. S. A. 108 (2011) 14121–14126.
[15] F. Minauro-Sanmiguel, S. Wilkens, J.J. Garcia, Structure of dimeric mitochondrial ATP synthase: novel F0 bridging features and the structural basis of mitochondrial cristae biogenesis, Proc. Natl. Acad. Sci. U. S. A. 102 (2005) 12356–12358.
[16] C. Bornhövd, F. Vogel, W. Neupert, A.S. Reichert, Mitochondrial membrane potential is dependent on the oligomeric state of F1F0-ATP synthase supracomplexes, J. Biol. Chem. 281 (2006) 13990–13998.
[17] M. Campanella, E. Casswell, S. Chong, Z. Farah, M.R. Wieckowski, A.Y. Abramov, A. Tinker, M.R. Duchen, Regulation of mitochondrial structure and function by the F1Fo-ATPase inhibitor protein, IF1, Cell. Metab. 8 (2008) 13–25.
[18] E. Bisetto, F. Di Pancrazio, M.P. Simula, I. Mavelli, G. Lippe, Mammalian ATPsynthase monomer versus dimer profiled by blue native PAGE and activity stain, Electrophoresis 28 (2007) 3178–3185.
[19] S.H. Ackerman, A. Tzagoloff, Function, structure, and biogenesis of mitochondrial ATP synthase, Prog. Nucleic Acid Res. Mol. Biol. 80 (2005) 95–133.
[20] L.A. Baker, I.N. Watt, M.J. Runswick, J.E. Walker, J.L. Rubinstein, Arrangement of subunits in intact mammalian mitochondrial ATP synthase determined by cryo-EM, Proc. Natl. Acad. Sci. U. S. A. 109 (2012) 11675–11680.
[21] H. Schägger, Respiratory chain supercomplexes of mitochondria and bacteria, Biochim. Biophys. Acta 1555 (2002) 154–159.
[22] I. Arnold, K. Pfeiffer, W. Neupert, R.A. Stuart, H. Schägger, Yeast mitochondrial F1F0-ATP synthase exists as a dimer: identification of three dimer-specific subunits, EMBO J. 17 (1998) 7170–7178.
[23] G. Arselin, J. Vaillier, B. Salin, J. Schaeffer, M.F. Giraud, A. Dautant, D. Brèthes, J. Velours, The modulation in subunits e and g amounts of yeast ATP synthase modifies mitochondrial cristae morphology, J. Biol. Chem. 279 (2004) 40392–40399.
[24] E. Bisetto, P. Picotti, V. Giorgio, V. Alverdi, I. Mavelli, G. Lippe, Functional and stoichiometric analysis of subunit e in bovine heart mitochondrial F(0)F(1)ATP synthase, J. Bioenerg. Biomembr. 40 (2008) 257–267.
[25] T. Weimann, J. Vaillier, B. Salin, J. Velours, The intermembrane space loop of subunit b (4) is a major determinant of the stability of yeast oligomeric ATP synthases, Biochemistry 47 (2008) 3556–3563.
[26] R. Fronzes, T. Weimann, J. Vaillier, J. Velours, D. Brèthes, The peripheral stalk participates in the yeast ATP synthase dimerization independently of e and g subunits, Biochemistry 45 (2006) 6715–6723.
[27] I. Wittig, I. Velours, R. Stuart, H. Schägger, Characterization of domain interfaces in monomeric and dimeric ATP synthase, Mol. Cell. Proteomics 7 (2008) 995–1004.
[28] S.J. Couoh-Cardel, S. Uribe-Carvajal, S. Wilkens, J.J. García-Trejo, Structure of dimeric F1F0-ATP synthase, J. Biol. Chem. 285 (2010) 36447–36455.
[29] K.M. Davies, C. Anselmi, I. Wittig, J.D. Faraldo-Gómez, W. Kühlbrandt, Structure of the yeast F1Fo-ATP synthase dimer and its role in shaping the mitochondrial cristae, Proc. Natl. Acad. Sci. U. S. A. 109 (2012) 13602–13607.
[30] D.W. Green, G.J. Grover, The IF(1) inhibitor protein of the mitochondrial F(1) F(0)-ATPase, Biochim. Biophys. Acta 1458 (2000) 343–355.
[31] F. Di Pancrazio, I. Mavelli, M. Isola, G. Losano, P. Pagliaro, D.A. Harris, G. Lippe, In vitro and in vivo studies of F(0)F(1)ATP synthase regulation by inhibitor protein IF(1) in goat heart, Biochim. Biophys. Acta 1659 (2004) 52–62.
[32] C. Penna, P. Pagliaro, R. Rastaldo, F. Di Pancrazio, G. Lippe, D. Gattullo, D. Mancardi, M. Samaja, G. Losano, I. Mavelli, F0F1 ATP synthase activity is differently modulated by coronary reactive hyperemia before and after ischemic preconditioning in the goat, Am. J. Physiol. Heart Circ. Physiol. 287 (2004) H2192–HG21200.
[33] J.J. García, E. Morales-Ríos, P. Cortés-Hernandez, J.S. Rodríguez-Zavala, The inhibitor protein (IF1) promotes dimerization of the mitochondrial F1F0-ATP synthase, Biochemistry 45 (2006) 12695–12703.
[34] D. De los Rios Castillo, M. Zarco-Zavala, S. Olvera-Sanchez, J.P. Pardo, O. Juarez, F. Martinez, G. Mendoza-Hernandez, J.J. García-Trejo, O. Flores-Herrera, Atypical cristae morphology of human syncytiotrophoblast mitochondria: role for complex V, J. Biol. Chem. 286 (2011) 23911–23919.
[35] L. Tomasetig, F. Di Pancrazio, D.A. Harris, I. Mavelli, G. Lippe, Dimerization of F0F1ATP synthase from bovine heart is independent from the binding of the inhibitor protein IF1, Biochim. Biophys. Acta 1556 (2002) 133–1441.
[36] Dienhart, K. Pfeiffer, H. Schagger, R.A. Stuart, Formation of the yeast F1F0-ATP synthase dimeric complex does not require the ATPase inhibitor protein, Inh1, J. Biol. Chem. 277 (2002) 39289–39295.
[37] R. Domenis, E. Bisetto, D. Rossi, M. Comelli, I. Mavelli, Glucose-modulated mitochondria adaptation in tumor cells: a focus on ATP synthase and inhibitor factor 1, Int. J. Mol. Sci. 13 (2012) 1933–1950.
[38] M.B. Hock, A. Kralli, Transcriptional control of mitochondrial biogenesis and function, Annu. Rev. Physiol. 71 (2009) 177–203.
[39] C.S. Kraft, C.M. LeMoine, C.N. Lyons, D. Michaud, C.R. Mueller, C.D. Moyes, Control of mitochondrial biogenesis during myogenesis, Am. J. Physiol. Cell Physiol. 290 (2006) C1119–C1127.
[40] L. Wilson-Fritch, A. Burkart, G. Bell, K. Mendelson, J. Leszyk, S. Ricoloro, Mitochondrial biogenesis and remodeling during adipogenesis and in response to the insulin sensitizer rosiglitazone, Mol. Cell. Biol. 23 (2003) 1085–1094.
[41] J.C. St John, J. Ramalho-Santos, H.L. Gray, P. Petrosko, V.Y. Rawe, C.S. Navara, C.R. Simerly, G.P. Schatten, The expression of mitochondrial DNA transcription factors during early cardiomyocyte in vitro differentiation from human embryonic stem cells, Cloning Stem Cells 7 (2005) 141–153.
[42] S. Chung, P.P. Dzeja, R.S. Faustino, C. Perez-Terzic, A. Behfar, A. Terzic, Mitochondrial oxidative metabolism is required for the cardiac differentiation of stem cells, Nat. Clin. Pract. Cardiovasc. Med. 4 (2007) S60–S67.
[43] M. Comelli, R. Domenis, E. Bisetto, M. Contin, M. Marchini, F. Ortolani, L. Tomasetig, I. Mavelli, Cardiac differentiation promotes mitochondria development and ameliorates oxidative capacity in H9c2 cardiomyoblasts, Mitochondrion 11 (2011) 315–326.
[44] N. San Martin, A.M. Cervera, C. Cordova, D. Covarello, K.J. McCreath, B.G. Galvez, Mitochondria determine the differentiation potential of cardiac mesoangioblasts, Stem Cells 29 (2011) 1064–1074.
[45] H. Schägger, G. von Jagow, Blue native electrophoresis for isolation of membrane protein complexes in enzymatically active form, Anal. Biochem. 199 (1991) 223–231.
[46] C. Ménard, S. Pupie, D. Mornet, M. Kitzmann, J. Nargeot, P. Lory, Modulation of L-type calcium channel expression during retinoic acid-induced differentiation of H9C2 cardiac cell, J. Biol. Chem. 274 (1999) 29063–29070.
[47] O.H. Lowry, N.J. Rosebrough, R.A. Lewis, R.J. Randall, Protein measurement with the folin phenol reagent, J. Biol. Chem. 193 (1951) 265–275.
[48] M. Comelli, G. Lippe, I. Mavelli, Differentiation potentiates oxidant injury to mitochondria by hydrogen peroxide in Friend's erythroleukemia cells, FEBS Lett. 352 (1994) 71–75.
[49] M.M. Bradford, A rapid and sensitive method for the quantitation of microgram quantities of protein utilizing the principle of protein-dye binding, Anal. Biochem. 72 (1976) 248–254.
[50] U.K. Laemmli, Cleavage of structural proteins during the assembly of the head of bacteriophage T4, Nature 227 (1970) 680–685.
[51] L.L. Horstman, E. Racker, Partial resolution of the enzyme catalyzing oxidative phosphorylation. Interaction between mitochondrial adenosine triphosphatase inhibitor and mitochondrial adenosine triphosphatase, J. Biol. Chem. 245 (1970) 1336–1344.
[52] J.C. Gomez-Fernandez, D.A. Harris, A thermodynamic analysis of the interaction between the mitochondrial coupling adenosine triphosphatase and its naturally occurring inhibitor protein, Biochem. J. 176 (1978) 967–975.
[53] A.M. Salzano, G. Renzone, A. Scaloni, A. Torreggiani, C. Ferreri, C. Chatgilialoglu, Human serum albumin modifications associated with reductive radical stress, Mol. Biosyst. 7 (2011) 889–898.
[54] J. Habersetzer, W. Ziani, I. Larrieu, C. Stines-Chaumeil, M.F. Giraud, D. Brèthes, A. Dautant, P. Paumard, ATP synthase oligomerization: from the enzyme models to the mitochondrial morphology, Int. J. Biochem. Cell Biol. 45 (2012) 99–105.
[55] A.S. Fandiño, I. Rais, M. Vollmer, H. Elgass, H. Schägger, M. Karas, LC–nanospray-MS/MS analysis of hydrophobic proteins from membrane protein complexes isolated by blue-native electrophoresis, J. Mass Spectrom. 40 (2005) 1223–1231.
[56] H.J. Wessels, R.O. Vogel, L. van den Heuvel, J.A. Smeitink, R.J. Rodenburg, L.G. Nijtmans, M.H. Farhoud, LC–MS/MS as an alternative for SDS-PAGE in blue native analysis of protein complexes, Proteomics 9 (2009) 4221–4228.
[57] I. Wittig, B. Meyer, H. Heide, M. Steger, L. Bleier, Z. Wumaier, M. Karas, H. Schägger, Assembly and oligomerization of human ATP synthase lacking mitochondrial subunits a and A6L, Biochim. Biophys. Acta 1797 (2010) 1004–1011.
[58] F. Zanotti, G. Raho, A. Gaballo, S. Papa, Inhibitory and anchoring domains in the ATPase inhibitor protein IF1 of bovine heart mitochondrial ATP synthase, J. Bioenerg. Biomembr. 36 (2004) 447–457.
[59] A.I. Jonckheere, J.A. Smeitink, R.J. Rodenburg, Mitochondrial ATP synthase: architecture, function and pathology, Inherit. Metab. Dis. 35 (2012) 211–225.
[60] I. Wittig, H. Schägger, Structural organization of mitochondrial ATP synthase, Biochim. Biophys. Acta 1777 (2008) 592–598.
[61] L. Formentini, M. Sanchez-Aragò, L. Sanchez-Cenizo, J.M. Cuezva, The mitochondrial ATPase Inhibitory factor 1 triggers a ROS-mediated retrograde prosurvival and proliferative response, Mol. Cell 45 (2012) 1–12.